Transport Theory for Topological Josephson Junctions with a Majorana Qubit

Zhi Wang,[1,2,*,†] Jia-Jin Feng,[3,†] Zhao Huang,[4,‡] and Qian Niu[5]
[1]*School of Physics, Sun Yat-sen University, Guangzhou 510275, China*
[2]*Guangdong Provincial Key Laboratory of Magnetoelectric Physics and Devices, Sun Yat-sen University, Guangzhou 510275, China*
[3]*International Center for Quantum Materials, Peking University, Beijing 100871, China*
[4]*Texas Center for Superconductivity, University of Houston, Houston, Texas 77204, USA*
[5]*School of Physical Sciences, University of Science and Technology of China, Hefei 230026, China*

(Received 26 April 2022; accepted 15 November 2022; published 16 December 2022)

We construct a semiclassical theory for the transport of topological Josephson junctions starting from a microscopic Hamiltonian that comprehensively includes the interplay among the Majorana qubit, the Josephson phase, and the dissipation process. With the path integral approach, we derive a set of semiclassical equations of motion that can be used to calculate the time evolution of the Josephson phase and the Majorana qubit. In the equations we reveal rich dynamical phenomena such as the qubit-induced charge pumping, the effective spin-orbit torque, and the Gilbert damping. We demonstrate the influence of these dynamical phenomena on the transport signatures of the junction. We apply the theory to study the Shapiro steps of the junction, and find the suppression of the first Shapiro step due to the dynamical feedback of the Majorana qubit.

DOI: 10.1103/PhysRevLett.129.257001

Introduction.—Josephson physics has received renewed interest due to the rapid progress of superconducting quantum computation in recent years [1,2]. The demand for the minification of the superconducting quantum circuits pushes the limits of the size of Josephson junctions [3,4]. For junctions that are small enough, a single embedded qubit may significantly modify the transport signatures [5]. While this effect has been discussed in a number of systems with various models [6–8], a comprehensive theory that takes into account the qubit dynamics is still absent.

This issue is particularly relevant to topological Josephson junctions with Majorana zero modes [9–35]. The two Majorana zero modes in the junction construct a Majorana qubit which results in a 4π-periodic Josephson current [36,37]. Previous theoretical studies take a variety of phenomenological models which are different extensions of the standard resistively shunted junction model for conventional junctions [6,7,38–42]. However, these phenomenological models still have difficulties in explaining the experimental reported transport features such as the suppression of the first Shapiro step [43–50]. It is highly desirable to construct a microscopic theory to examine the validity of the phenomenological models and to understand the experimental results.

In this Letter, we develop a semiclassical theory for studying the transport properties of the topological junctions. Our theory starts from a microscopic Hamiltonian that characterizes the coupling between the Josephson junction and the Majorana qubit. We take a path integral approach to incorporate the dissipation process that is essential for studying the transport properties and derive the semiclassical equations of motion for the Josephson phase and the Majorana qubit. In the equations of motion, we identify the effective spin-orbit torque and the Gilbert damping in the qubit dynamics and reveal the charge pumping driven by the qubit rotation in the dynamics of the Josephson phase. Solving the equations of motion, we obtain the time evolution of the Josephson phase which provides transport and spectroscopic signatures for the junction.

As an application of this theory, we calculate the Shapiro steps of the topological junction. We find that the first step is strongly suppressed while higher odd-number steps are robustly visible for a range of junction parameters. We show that this bizarre behavior is due to the feedback of the Majorana qubit dynamics to the transport of the junction. At the voltage of the first step, the Majorana qubit evolves to a stable state which supports a finite 4π-period Josephson current, and this 4π periodicity in the Josephson phase dynamics suppresses the first Shapiro step. At voltages of higher odd-number steps, however, the Majorana qubit evolves to a stable state which contributes a vanishing 4π-period Josephson current, and the Shapiro steps are naturally intact. Our theory provides an intrinsic mechanism for the reported Shapiro step missing in topological junctions.

Microscopic Hamiltonian and equations of motion.—The low-energy effective Hamiltonian for the junction with a Majorana qubit can be written as [51]

$$\mathcal{H}_J = \frac{\hat{p}_\theta^2}{C_0} - E_J \cos\hat{\theta} - I_{\rm ex}\hat{\theta} - E_M \sigma_z \cos\frac{\hat{\theta}}{2} + E'_M \sigma_x, \quad (1)$$

where $\hat{\theta}$ is the Josephson phase with canonical momentum $\hat{p}_\theta = -i\partial_\theta$, E_J is the Josephson energy, $C_0 = 2C/(2e)^2$ is determined by the effective capacitance C of the junction (set $\hbar = 1$), $I_{\rm ex}$ represents the experimentally controllable external current injected into the junction, $\sigma_{x,z}$ are Pauli matrices which represent the pseudo-spin direction for the Majorana qubit, E_M and E_M' represent the energies of the Majorana qubit from various couplings between Majorana zero modes. The first three terms of the Hamiltonian have been widely adopted for studying conventional Josephson junctions [5], while the last two terms come from the Majorana zero modes [36,52] and can be derived from the Bogoliubov–de Gennes Hamiltonian of a topological Josephson junction [53,54].

This Hamiltonian can be understood as describing a spin-one-half *particle* with a mass of C_0, moving under a potential energy $U_p = -E_J\cos\theta - I_{\rm ex}\theta$, and a Zeeman energy $U_z = \mathbf{h}\cdot\hat{\sigma}$, where the direction of the Zeeman field $\mathbf{h} = [E_M', 0, -E_M\cos(\theta/2)]$ varies along the path of the motion. The potential energy is identical to the tilted-washboard potential that was taken in studying conventional junctions [5], while the unique Zeeman energy comes from the coupling between the Josephson phase and the Majorana qubit.

The time evolution of the Josephson phase determines the transport properties of the junction through the ac Josephson relation [55]. To derive the equation of motion for this time evolution, we rewrite the Hamiltonian of Eq. (1) into an action [51,56,57],

$$S_J = \int dt\left(\frac{C_0}{2}\dot{\theta}^2 + E_J\cos\theta + I_{\rm ex}\theta + \mathbf{A}_s\cdot\dot{\mathbf{s}} + \mathbf{h}\cdot\mathbf{s}\right), \qquad (2)$$

where $\mathbf{s} = \psi^\dagger\hat{\boldsymbol{\sigma}}\psi = (\sin\varphi\sin\phi, \sin\varphi\cos\phi, \cos\varphi)$ represents the psuedo-spin state on the Bloch sphere with $\psi = [e^{-i\phi}\cos(\varphi/2), \sin(\varphi/2)]$ the spinor wave function of the qubit, $\mathbf{A}_s = \hat{\mathbf{e}}_\phi(1-\cos\varphi)/\sin\varphi$ represents the Berry connection on the Bloch sphere [57], which provides a Berry curvature of $\nabla\times\mathbf{A}_s = \mathbf{s}$. The extreme action path of Eq. (2) gives the semiclassical equations of motion for the Josephson phase $C\ddot{\theta}/2e + I_{c1}\sin\theta + I_{c2}s_z\sin(\theta/2) - I_{\rm ex} = 0$, and the pseudo-spin $\dot{\mathbf{s}} = \mathbf{h}\times\mathbf{s}$, where $I_{c1} = 2eE_J/\hbar$ is the supercurrent from the Cooper pair tunneling and $I_{c2} = eE_M/\hbar$ is the supercurrent from the half-pair tunneling through the Majorana qubit. The equations of motion explicitly demonstrate the coupling between the Josephson phase and the Majorana qubit through the s_z-dependent Zeeman term in the first equation and the θ-dependent effective magnetic field in the second equation. However, these equations are inadequate for studying the transport properties of the junction. The missing piece is the dissipation process.

To include the dissipation into the equations of motion [58–60], we follow the Caldeira-Leggett approach and introduce a thermal bath of harmonic modes to characterize the environment [61,62]. The environmental degrees of freedom and their coupling with the junction can be described with the action [51]

$$S_{\rm en} = \sum_i \int dt\left[\frac{1}{2}(\dot{h}_i^2 - \Omega_i^2 h_i^2) + h_i(g_i\theta + \mathbf{B}_i\cdot\mathbf{s})\right], \qquad (3)$$

where h_i are the coordinates of the environmental modes and Ω_i are their oscillating energies, g_i represents the minimal coupling between the environmental modes and the Josephson phase [62], and $\mathbf{B}_i$ represents the minimal coupling between the environmental modes and the qubit [63]. The details of g_i and $\mathbf{B}_i$ are determined by the coupling between each environmental mode and the junction. For topological junctions described by Eq. (1), the environmental modes that modulate the tunneling barrier of the junction can be understood as a fluctuation on the amplitude of E_M and we have $\mathbf{B}_i = B_i\hat{z}$, while the environmental modes that modulate the coupling between Majorana zero modes in one side of the junction can be understood as a fluctuation on E_M' and we have $\mathbf{B}_i = B_i\hat{x}$.

The dissipated evolution of the junction can be obtained by integrating out the environmental degrees of freedom. This is achievable since the environment is modeled with harmonic modes. After the integration, we arrive at an effective action for the junction variables [51],

$$S_{\rm eff} = \int dt\left(\frac{C_0}{2}\dot{\theta}^2 + E_J\cos\theta + I_{\rm ex}\theta + \mathbf{A}_s\cdot\dot{\mathbf{s}} + \mathbf{h}\cdot\mathbf{s}\right) + \frac{1}{4}\int dt dt'[\eta_\alpha(t) - \eta_\alpha(t')]G_{\alpha\beta}(t,t')[\eta_\beta(t) - \eta_\beta(t')], \qquad (4)$$

where $\eta_\alpha = (\theta, s_x, s_y, s_z)$ represents the junction degree of freedom, and $G_{\alpha\beta}(t,t') = -i(\tilde{M}/\pi)(1/|t-t'|^2)$ is the averaged Green function from the environmental modes, with $\tilde{M}$ the averaged coupling matrix [51]. The least action path for this effective action provides the full semiclassical equations of motion for the junction variables,

$$I_{\rm ex} = C\ddot{\theta} + \frac{\dot{\theta}}{R} + I_{c1}\sin\theta + I_{c2}s_z\sin\frac{\theta}{2} + \mathbf{B}_f\cdot\dot{\mathbf{s}}, \qquad (5a)$$

$$\dot{\mathbf{s}} = \mathbf{h}\times\mathbf{s} + \dot{\theta}\mathbf{B}_f\times\mathbf{s} + (\tilde{\gamma}\cdot\dot{\mathbf{s}})\times\mathbf{s}, \qquad (5b)$$

where $R = 1/\sum_i g_i^2$ is the effective resistance of the junction which comes from the coupling between the environment and the Josephson phase, $\mathbf{B}_f = \sum_i g_i\mathbf{B}_i$ is the environment mediated coupling field between the Josephson phase and the qubit, and $\tilde{\gamma}_{\alpha\beta} = \sum_i B_{i\alpha}B_{i\beta}$ represents the environment-induced dissipation to the qubit.

Equation (5) is the central result of this Letter. Solving these two self-consistent equations we can obtain $\theta(t)$

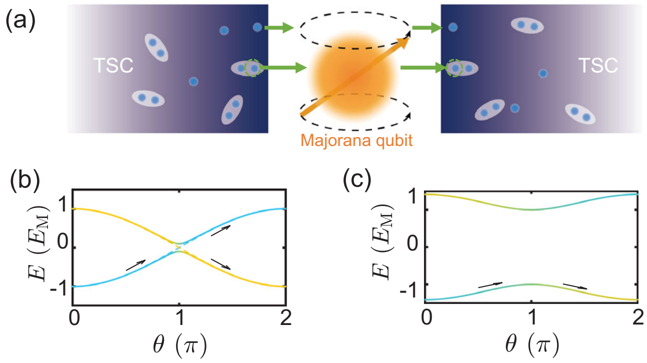

FIG. 1. (a) Schematic illustration of two tunneling processes through the Majorana qubit: the qubit assisted half-pair tunneling that leads to the fractional Josephson effect and the qubit rotation induced charge pumping. (b) The energy levels of the Hamiltonian $\mathbf{h}\cdot\hat{\sigma}$. Landau-Zener transitions happen at the anticrossing points at $\theta=(2n+1)\pi$. (c) The energy levels of the Hamiltonian $(\mathbf{h}+\dot{\theta}\mathbf{B}_f)\cdot\hat{\sigma}$ for high voltage of $\dot{\theta}\gg E_M/B_f$, where $\mathbf{B}_f=B_f\hat{x}$. The Landau-Zener transition at the anticrossing points are significantly suppressed and the qubit dynamics would follow one of the levels.

which determines the dc and ac voltage of the junction through the Josephson relation $V(t)=\hbar\dot{\theta}(t)/2e$. Starting from a microscopic Hamiltonian, we provide a framework to study the transport properties of a Josephson junction with an embedded Majorana qubit.

Physical interpretation of the equations of motion.—Let us set up a physical picture for interpreting the terms in the equations of motion, particularly those terms coming from the embedded Majorana qubit. Equation (5a) is a current conservation equation which states that the externally injected current I_{ex} equals the current flowing through all the physical channels in the junction. If the qubit is completely ignored, then the last two terms on the right-hand side of Eq. (5a) should be dropped out and the equation becomes a self-consistent equation for the Josephson phase. This is exactly the resistively and capacitively shunted junction model that has been widely used for studying bulk Josephson junctions [5].

The qubit provides two additional terms in Eq. (5a) as illustrated in Fig. 1(a). The first term is the 4π-periodic Josephson current $I_{c2}s_z\sin(\theta/2)$, which is linearly dependent on the z component of the pseudo-spin. This is the extensively discussed fractional Josephson effect [36,53,64], which comes from the qubit assisted half-pair tunneling in the junction. The other term is $\mathbf{B}_f\cdot\dot{\mathbf{s}}$ which is nonvanishing only when the pseudo-spin rotates. Since the pseudo-spin state of the Majorana qubit is defined by the parity of the superconducting ground state, this current represents the pumped current by the parity flipping of the Majorana qubit. This qubit pumping has never been revealed in previous models, and only becomes apparent from the effective action of the microscopic theory.

Now we take a closer look at Eq. (5b). In the absence of the environment, only the first term on the right-hand side of the equation survives. The residing equation, $\dot{\mathbf{s}}=\mathbf{h}\times\mathbf{s}$, describes a qubit precession where the direction of the precession $\mathbf{h}$ oscillates with θ. When the oscillating component h_z is much larger than the stable component h_x, the qubit would evolve under an oscillating energy spectrum shown in Fig. 1(b). This evolution can be understood with the Landau-Zener transitions which happen at the anticrossing points $\theta=(2n+1)\pi$. Multiple coherent Landau-Zener transitions can exhibit Stückelburg interference [6,65,66]. Meanwhile, the evolution can also be characterized with the instantaneous eigenstates of $\mathbf{h}\cdot\hat{\sigma}$, where additional $\dot{\theta}$ linear Berry connection contributions would appear [51,67,68].

The second term on the right-hand side of Eq. (5b) is a unique discovery of our theory. It resembles a spin-orbit torque which linearly depends on the velocity of the Josephson phase. This spin-orbit torque dominates the qubit dynamics at high voltage of $\dot{\theta}\gg E'_M/\hbar$, causing a significant suppression of the energy crossing and the Landau-Zener transition, as shown in Fig. 1(c). For this reason, the transport and spectroscopic signals of the junction are expected to exhibit qualitatively different behaviors for different voltage regimes. This is useful for understanding the voltage-dependent signatures that have been widely reported in the I-V characteristics curves and Josephson radiations of Josephson junctions constructed by topological systems [10,13,22].

The third term on the right-hand side of Eq. (5b) is the anisotropic Gilbert damping which determines the dissipation of the qubit from the coupling to the environment. For the isotropic case where the matrix $\tilde{\gamma}$ becomes a number, this term turns into the standard Gilbert damping which appeared in the Landau-Lifshiz-Gilbert equation [69]. While the Gilbert damping has been widely taken to study the dynamics of the magnetization, our Letter provides a derivation for its appearance in topological junctions with a Majorana qubit. This damping process influences the dynamics of the qubit and thereby modifies the transport properties of the junction.

We note that our theory is not only useful for calculating transport properties. It can also be used to study dynamical features of the junction such as the Josephson radiation. Also, the qubit pumping suggests a novel current flow from the dynamics of Majorana qubit. These features might be useful for experimental measurement of the quantum rotation of the Majorana qubit. Finally, we hope to point out that if the environment mediated coupling $\mathbf{B}_f$ and the Gilbert damping $\tilde{\gamma}$ are ignored, then Eq. (5) will reduce to the phenomenological quantum resistively and capacitively shunted junction model that has been taken to study the I-V characteristics and the Josephson radiations of the topological junction [6,66]. Our microscopic theory clarifies the validity and limits of the phenomenological model.

Fixed point analysis.—Equations (5) are complicated nonlinear equations for which obtaining analytical solutions is impossible. However, the fixed points of the equations can be analytically calculated with the method of averaging, which is a method to decouple the nonlinear equations with the division of the dynamical variables to the "fast variables" and the "slow variables" based on their timescales [70]. In Eq. (5) we treat the pseudo-spin $\mathbf{s}$ as the slow variable since it has a larger timescale. We take it as constant to solve Eq. (5a) for the fast variable $\theta(t)$, and the solution provides the time-averaged Josephson energy $\int dt E_M \cos\theta(t)/2 \approx \alpha s_z E_M$. Plugging this into Eq. (5b), we obtain an approximated self-consistent equation for $\mathbf{s}$, and the fixed points of this equation can be determined analytically. There are two sets of fixed points. The first is the trivial fixed points at $\mathbf{s}_0 = \pm(1,0,0)$ which are stable fixed points for all parameters. If the system evolves toward these fixed points, the 4π-periodic Josephson current in Eq. (5a) vanishes and all experimental 4π-periodic signatures would disappear. The other set of fixed points locates at [51]

$$\mathbf{s}_1 = \pm[(E'_M + V_0 B_f)/E_M\alpha, 0, \sqrt{1-(E'_M+V_0B_f)^2/E_M^2\alpha^2}], \tag{6}$$

which are stable fixed points only when the injected current is small so that the dc voltage is smaller than a critical value of $V_c = |E_M\alpha - E'_M|/B_f$. For quantum spin Hall insulator junction [45], it is estimated to be around 10–100 μV [51]. The existence of these fixed points is voltage dependent, which is qualitatively different from the trivial fixed points.

These analytical results for fixed points provide insight into the experimentally reported voltage-dependent behaviors of topological junctions [10,13]. From the fixed point analysis, we find two different voltage regimes. At dc voltage below V_c, there are two sets of fixed points, and the system has a chance of evolving to either of them. If the system evolves to the fixed point $\mathbf{s}_1$ as shown in Fig. 2(a), the final stable state would have a nonvanishing s_z and therefore a nonvanishing 4π-periodic Josephson current shows up in the equation for the Josephson phase. In this voltage regime, we should expect transport signatures for 4π periodicity. However, for the voltage above V_c, there exits only the trivial fixed points at $\mathbf{s}_0$. When the system evolves toward it as shown in Fig. 2(b), the final stable state would have a vanishing s_z, and the 4π-periodic Josephson current vanishes. In this voltage regime, all the transport signatures for the 4π periodicity should disappear. Based on this fixed point analysis, we predict that the transport of topological junctions would exhibit nontrivial 4π-periodic signatures only at low voltage, while at high voltages it would look quite similar to the trivial junctions.

Shapiro steps.—The Shapiro steps are the plateaus of the I-V curve at voltages $V_n = n\hbar\omega/2e$ under an injected ac current with frequency ω. It is a powerful tool for probing the dynamics of Josephson junctions since it reflects the resonance between the dc and the ac Josephson relation.

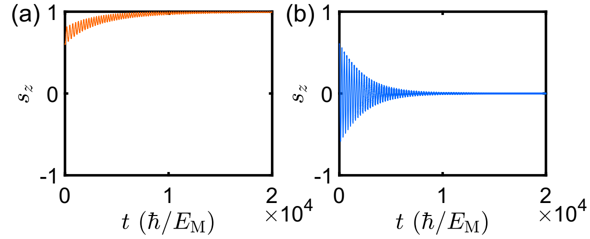

FIG. 2. Typical time evolution of the Majorana qubit for (a) the low voltage regime of $V < V_c$ and (b) the high voltage regime of $V > V_c$. The damped oscillations are combined effect of the Landau-Zener-Stückelburg interference and the Gilbert damping. The two different stable values of the s_z represent the different fixed points in the dynamics of the Majorana qubit. Parameters of the junction are taken as $E'_M/E_M = 0.01$, $I_{c1}/I_{c2} = 0.5$, $2eI_{c2}R/E_M = 0.5$, $\mathbf{B}_f = 0.01\hat{x}$.

For topological junctions, it was anticipated that the odd-number Shapiro steps with $n = 1, 3, 5\ldots$ should be suppressed by the 4π-periodic supercurrent. The experimental results, however, often show strong suppression of low order odd-number steps such as the one with $n = 1$, while other odd-number Shapiro steps at higher voltages are robust. Since the understanding of the experimental results is crucial for detecting Majorana zero modes, it is timely to implement Eq. (5) to calculate the Shapiro steps of Majorana Josephson junctions.

We consider an injected current of $I_{\rm ex}(t) = I + I'\cos\omega t$ and calculate the I-V curve of the junction, with the results for a typical junction parameter shown in Fig. 3(a). We find

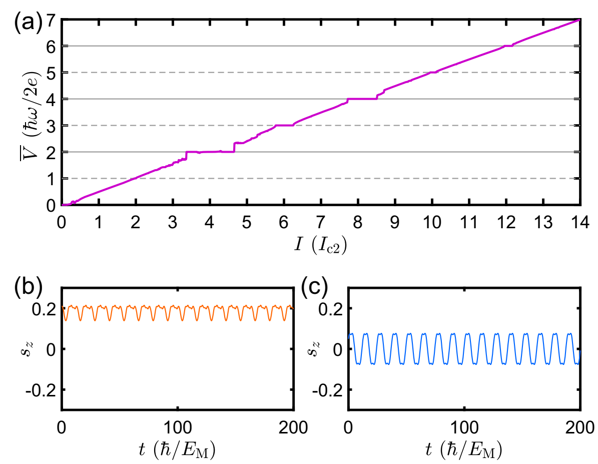

FIG. 3. (a) The Shapiro steps for the topological Josephson junction simulated with Eq. (5). The first Shapiro step is strongly suppressed while all other steps are clearly visible. (b) The time evolution of s_z for the voltage around the first Shapiro step. The pseudo-spin oscillates with a nonzero averaging value, and the resulted 4π-periodic supercurrent strongly suppresses the first step. (c) The time evolution of s_z for the voltage around the third Shapiro step. The pseudo-spin goes to the fixed point of $s_z \approx 0$ which effectively shuts down the 4π-periodic channel for the Josephson current. Parameters are taken as $\omega/E_M = 1$, $I'/I_{c2} = 8$ with other parameters taken the same as in Fig. 2.

Shapiro steps at $V = n\hbar\omega/2e$, where n labels the number of the step. Intriguingly, it is clear that the first Shapiro step with $n = 1$ is strongly suppressed, while all other steps are clearly visible. At first glance, the suppression of only one Shapiro step seems mysterious. One would expect a suppression of all odd-number steps if the 4π-periodic supercurrent carried by the Majorana qubit is significant, or no suppression to any of the steps if the 4π-periodic supercurrent is irrelevant. For this phenomenon, our theory provides a possible mechanism: the feedback from the dynamics of the Majorana qubit. As we have shown in the analytical results, the Majorana qubit evolves to different stable states for different voltages. We examine the qubit dynamics at the voltages for the first step and the third step. As shown in Fig. 3(b), at the voltage where the first step should appear, the Majorana qubit evolves to the stable state with a finite s_z. Then the 4π-periodic Josephson current will dominate and the Shapiro step is suppressed. For the higher voltage of the third step, however, the Majorana qubit evolves to a stable state with $s_z \approx 0$, as shown in Fig. 3(c). Then the 4π-periodic supercurrent is blocked, and the junction would behave similar to a conventional junction presenting Shapiro steps. This feedback of the qubit dynamics provides a simple mechanism for the suppression of the first Shapiro step, and gives a possible explanation to one of the puzzles in the experimental findings of topological superconductors.

We emphasize that, while our theory is derived for topological junctions with Majorana qubit, it is actually valid for any junction with an embedded qubit that can be described by the low-energy effective Hamiltonian Eq. (1). One such example is the Josephson junction with quantum dots [8]. In this sense, our calculation of Shapiro steps provides a signal for the feedback of an embedded qubit, instead of a unique signature of Majorana zero modes.

Conclusion.—In summary, we constructed a semiclassical theory for the topological Josephson junctions with an embedded Majorana qubit. We revealed nontrivial qubit dynamics such as the Landau-Zener transitions and the anisotropic Gilbert damping. We found that the feedback of the qubit dynamics strongly modifies the transport features of the junction. We applied the theory to study the Shapiro steps of the topological junctions and demonstrated the suppression of the first Shapiro step which agrees with recent experiments. We reveal that this phenomenon is due to the voltage-selective feedback from the dynamics of Majorana qubit.

We thank Zhongbo Yan, Peng Ye, and Shuai Yin for valuable discussions. This work was supported by the National Natural Science Foundation of China (Grants No. 12174453, No. 12234017, and No. 11774435), NKRDPC-2017YFA0206203, 2017YFA0303302, 2018YFA0305603, and Guangdong Basic and Applied Basic Research Foundation (Grant No. 2019A1515011620). Z. H. is supported by the Robert A. Welch Foundation under Grant No. E-1146.

*wangzh356@mail.sysu.edu.cn
†These authors contributed equally to this work.
‡huangzhaophysics@gmail.com

[1] M. H. Devoret and R. J. Schoelkopf, Superconducting circuits for quantum information: An outlook, Science **339**, 1169 (2013).

[2] J. M. Martinis, M. H. Devoret, and J. Clarke, Quantum Josephson junction circuits and the dawn of artificial atoms, Nat. Phys. **16**, 234 (2020).

[3] M. Kjaergaard, M. E. Schwartz, J. Braumüller, P. Krantz, J. I.-J. Wang, S. Gustavsson, and W. D. Oliver, Superconducting qubits: Current state of play, Annu. Rev. Condens. Matter Phys. **11**, 369 (2020).

[4] I. Siddiqi, Engineering high-coherence superconducting qubits, Nat. Rev. Mater. **6**, 875 (2021).

[5] M. Tinkham, *Introduction to Superconductivity* (Courier Corporation, New York, 2004).

[6] J.-J. Feng, Z. Huang, Z. Wang, and Q. Niu, Hysteresis from nonlinear dynamics of Majorana modes in topological Josephson junctions, Phys. Rev. B **98**, 134515 (2018).

[7] S.-J. Choi, A. Calzona, and B. Trauzettel, Majorana-induced dc Shapiro steps in topological Josephson junctions, Phys. Rev. B **102**, 140501(R) (2020).

[8] D. O. Oriekhov, Y. Cheipesh, and C. W. J. Beenakker, Voltage staircase in a current-biased quantum-dot Josephson junction, Phys. Rev. B **103**, 094518 (2021).

[9] M. T. Deng, C. L. Yu, G. Y. Huang, M. Larsson, P. Caroff, and H. Q. Xu, Anomalous zero-bias conductance peak in a Nb–InSb nanowire–Nb hybrid device, Nano Lett. **12**, 6414 (2012).

[10] J. B. Oostinga, L. Maier, P. Schüffelgen, D. Knott, C. Ames, C. Brüne, G. Tkachov, H. Buhmann, and L. W. Molenkamp, Josephson Supercurrent through the Topological Surface States of Strained Bulk HgTe, Phys. Rev. X **3**, 021007 (2013).

[11] Y. Peng, Y. Vinkler-Aviv, P. W. Brouwer, L. I. Glazman, and F. von Oppen, Parity Anomaly and Spin Transmutation in Quantum Spin Hall Josephson Junctions, Phys. Rev. Lett. **117**, 267001 (2016).

[12] J. Cayao, P. San-Jose, A. M. Black-Schaffer, R. Aguado, and E. Prada, Majorana splitting from critical currents in Josephson junctions, Phys. Rev. B **96**, 205425 (2017).

[13] R. S. Deacon, J. Wiedenmann, E. Bocquillon, F. Domínguez, T. M. Klapwijk, P. Leubner, C. Brüne, E. M. Hankiewicz, S. Tarucha, K. Ishibashi, H. Buhmann, and L. W. Molenkamp, Josephson Radiation from Gapless Andreev Bound States in HgTe-Based Topological Junctions, Phys. Rev. X **7**, 021011 (2017).

[14] F. Setiawan, W. S. Cole, J. D. Sau, and S. Das Sarma, Conductance spectroscopy of nontopological-topological superconductor junctions, Phys. Rev. B **95**, 020501(R) (2017).

[15] F. Setiawan, W. S. Cole, J. D. Sau, and S. Das Sarma, Transport in superconductor–normal metal–superconductor tunneling structures: Spinful p-wave and spin-orbit-coupled topological wires, Phys. Rev. B **95**, 174515 (2017).

[16] H. Kamata, R. S. Deacon, S. Matsuo, K. Li, S. Jeppesen, L. Samuelson, H. Q. Xu, K. Ishibashi, and S. Tarucha, Anomalous modulation of Josephson radiation in nanowire-based Josephson junctions, Phys. Rev. B **98**, 041302(R) (2018).

[17] C. Schrade and L. Fu, Parity-Controlled 2π Josephson Effect Mediated by Majorana Kramers Pairs, Phys. Rev. Lett. **120**, 267002 (2018).
[18] C. Lei, H. Chen, and A. H. MacDonald, Ultrathin Films of Superconducting Metals as a Platform for Topological Superconductivity, Phys. Rev. Lett. **121**, 227701 (2018).
[19] R. M. Lutchyn, E. P. A. M. Bakkers, L. P. Kouwenhoven, P. Krogstrup, C. M. Marcus, and Y. Oreg, Majorana zero modes in superconductor-semiconductor heterostructures, Nat. Rev. Mater. **3**, 52 (2018).
[20] Y.-H. Li, J. Song, J. Liu, H. Jiang, Q.-F. Sun, and X. C. Xie, Doubled Shapiro steps in a topological Josephson junction, Phys. Rev. B **97**, 045423 (2018).
[21] F. Liu, H.-Y. Deng, and K. Wakabayashi, Helical Topological Edge States in a Quadrupole Phase, Phys. Rev. Lett. **122**, 086804 (2019).
[22] D. Laroche, D. Bouman, D. J. van Woerkom, A. Proutski, C. Murthy, D. I. Pikulin, C. Nayak, R. J. J. van Gulik, J. Nygård, P. Krogstrup, L. P. Kouwenhoven, and A. Geresdi, Observation of the $4p$-periodic Josephson effect in indium arsenide nanowires, Nat. Commun. **10**, 245 (2019).
[23] C.-A. Li, J. Li, and S.-Q. Shen, Majorana-Josephson interferometer, Phys. Rev. B **99**, 100504(R) (2019).
[24] H. Ren, F. Pientka, S. Hart, A. T. Pierce, M. Kosowsky, L. Lunczer, R. Schlereth, B. Scharf, E. M. Hankiewicz, L. W. Molenkamp, B. I. Halperin, and A. Yacoby, Topological superconductivity in a phase-controlled Josephson junction, Nature (London) **569**, 93 (2019).
[25] A. Fornieri, A. M. Whiticar, F. Setiawan, E. Portolés, A. C. C. Drachmann, A. Keselman, S. Gronin, C. Thomas, T. Wang, R. Kallaher, G. C. Gardner, E. Berg, M. J. Manfra, A. Stern, C. M. Marcus, and F. Nichele, Evidence of topological superconductivity in planar Josephson junctions, Nature (London) **569**, 89 (2019).
[26] J. J. He, T. Liang, Y. Tanaka, and N. Nagaosa, Platform of chiral Majorana edge modes and its quantum transport phenomena, Commun. Phys. **2**, 149 (2019).
[27] A. Stern and E. Berg, Fractional Josephson Vortices and Braiding of Majorana Zero Modes in Planar Superconductor-Semiconductor Heterostructures, Phys. Rev. Lett. **122**, 107701 (2019).
[28] R. L. Klees, G. Rastelli, J. C. Cuevas, and W. Belzig, Microwave Spectroscopy Reveals the Quantum Geometric Tensor of Topological Josephson Matter, Phys. Rev. Lett. **124**, 197002 (2020).
[29] J. Ávila, E. Prada, P. San-Jose, and R. Aguado, Superconducting islands with topological Josephson junctions based on semiconductor nanowires, Phys. Rev. B **102**, 094518 (2020).
[30] D. Razmadze, E. C. T. O'Farrell, P. Krogstrup, and C. M. Marcus, Quantum Dot Parity Effects in Trivial and Topological Josephson Junctions, Phys. Rev. Lett. **125**, 116803 (2020).
[31] B. Scharf, A. Braggio, E. Strambini, F. Giazotto, and E. M. Hankiewicz, Thermodynamics in topological Josephson junctions, Phys. Rev. Res. **3**, 033062 (2021).
[32] M. C. Dartiailh, W. Mayer, J. Yuan, K. S. Wickramasinghe, A. Matos-Abiague, I. Žutić, and J. Shabani, Phase Signature of Topological Transition in Josephson Junctions, Phys. Rev. Lett. **126**, 036802 (2021).
[33] C.-Z. Li, A.-Q. Wang, C. Li, W.-Z. Zheng, A. Brinkman, D.-P. Yu, and Z.-M. Liao, Topological Transition of Superconductivity in Dirac Semimetal Nanowire Josephson Junctions, Phys. Rev. Lett. **126**, 027001 (2021).
[34] S.-K. Jian and S. Yin, Chiral topological superconductivity in Josephson junctions, Phys. Rev. B **103**, 134514 (2021).
[35] R.-X. Zhang and S. Das Sarma, Anomalous Floquet Chiral Topological Superconductivity in a Topological Insulator Sandwich Structure, Phys. Rev. Lett. **127**, 067001 (2021).
[36] A. Kitaev, Unpaired Majorana fermions in quantum wires, Phys. Usp. **44**, 131 (2001).
[37] H.-J. Kwon, K. Sengupta, and V. M. Yakovenko, Fractional ac Josephson effect in p- and d-wave superconductors, Eur. Phys. J. B **37**, 349 (2004).
[38] F. Domínguez, F. Hassler, and G. Platero, Dynamical detection of Majorana fermions in current-biased nanowires, Phys. Rev. B **86**, 140503(R) (2012).
[39] F. Domínguez, O. Kashuba, E. Bocquillon, J. Wiedenmann, R. S. Deacon, T. M. Klapwijk, G. Platero, L. W. Molenkamp, B. Trauzettel, and E. M. Hankiewicz, Josephson junction dynamics in the presence of 2π- and 4π-periodic supercurrents, Phys. Rev. B **95**, 195430 (2017).
[40] J. D. Sau and F. Setiawan, Detecting topological superconductivity using low-frequency doubled Shapiro steps, Phys. Rev. B **95**, 060501(R) (2017).
[41] A. E. Svetogorov, D. Loss, and J. Klinovaja, Critical current for an insulating regime of an underdamped current-biased topological Josephson junction, Phys. Rev. Res. **2**, 033448 (2020).
[42] D. Frombach and P. Recher, Quasiparticle poisoning effects on the dynamics of topological Josephson junctions, Phys. Rev. B **101**, 115304 (2020).
[43] L. P. Rokhinson, X. Liu, and J. K. Furdyna, The fractional a.c. Josephson effect in a semiconductor-superconductor nanowire as a signature of Majorana particles, Nat. Phys. **8**, 795 (2012).
[44] J. Wiedenmann, E. Bocquillon, R. S. Deacon, S. Hartinger, O. Herrmann, T. M. Klapwijk, L. Maier, C. Ames, C. Brüne, C. Gould, A. Oiwa, K. Ishibashi, S. Tarucha, H. Buhmann, and L. W. Molenkamp, $4p$-periodic Josephson supercurrent in HgTe-based topological Josephson junctions, Nat. Commun. **7**, 10303 (2016).
[45] E. Bocquillon, R. S. Deacon, J. Wiedenmann, P. Leubner, T. M. Klapwijk, C. Brüne, K. Ishibashi, H. Buhmann, and L. W. Molenkamp, Gapless Andreev bound states in the quantum spin Hall insulator HgTe, Nat. Nanotechnol. **12**, 137 (2017).
[46] C. Li, J. C. de Boer, B. de Ronde, S. V. Ramankutty, E. van Heumen, Y. Huang, A. de Visser, A. A. Golubov, M. S. Golden, and A. Brinkman, 4π-periodic Andreev bound states in a Dirac semimetal, Nat. Mater. **17**, 875 (2018).
[47] A.-Q. Wang, C.-Z. Li, C. Li, Z.-M. Liao, A. Brinkman, and D.-P. Yu, 4π-Periodic Supercurrent from Surface States in Cd_3As_2 Nanowire-Based Josephson Junctions, Phys. Rev. Lett. **121**, 237701 (2018).
[48] P. Schüffelgen, D. Rosenbach, C. Li, T. W. Schmitt, M. Schleenvoigt, A. R. Jalil, S. Schmitt, J. Kölzer, M. Wang,

B. Bennemann, U. Parlak, L. Kibkalo, S. Trellenkamp, T. Grap, D. Meertens, M. Luysberg, G. Mussler, E. Berenschot, N. Tas, A. A. Golubov, A. Brinkman, T. Schäpers, and D. Grützmacher, Selective area growth and stencil lithography for in situ fabricated quantum devices, Nat. Nanotechnol. **14**, 825 (2019).

[49] K. Le Calvez, L. Veyrat, F. Gay, P. Plaindoux, C. B. Winkelmann, H. Courtois, and B. Sacépé, Joule overheating poisons the fractional ac Josephson effect in topological Josephson junctions, Commun. Phys. **2**, 4 (2019).

[50] D. Rosenbach, T. W. Schmitt, P. Schüffelgen, M. P. Stehno, C. Li, M. Schleenvoigt, A. R. Jalil, G. Mussler, E. Neumann, S. Trellenkamp, A. A. Golubov, A. Brinkman, D. Grützmacher, and T. Schäpers, Reappearance of first Shapiro step in narrow topological Josephson junctions, Sci. Adv. **7**, eabf1854 (2021).

[51] See Supplemental Materials at http://link.aps.org/supplemental/10.1103/PhysRevLett.129.257001 for the detailed derivation of the semiclassical equations for the Josephson phase and the pseudo-spin, the analytical treatment based on method of averaging, and the Berry connection contribution in the near adiabatic processes.

[52] A. Y. Kitaev, Fault-tolerant quantum computation by anyons, Ann. Phys. (Amsterdam) **303**, 2 (2003).

[53] R. M. Lutchyn, J. D. Sau, and S. Das Sarma, Majorana Fermions and a Topological Phase Transition in Semiconductor-Superconductor Heterostructures, Phys. Rev. Lett. **105**, 077001 (2010).

[54] Y. Oreg, G. Refael, and F. von Oppen, Helical Liquids and Majorana Bound States in Quantum Wires, Phys. Rev. Lett. **105**, 177002 (2010).

[55] B. D. Josephson, Possible new effects in superconductive tunnelling, Phys. Lett. **1**, 251 (1962).

[56] X.-G. Wen, Quantum field theory of many-body systems from the origin of sound to an origin of light and electrons, *Quantum Field Theory of Many-body Systems* (Oxford University Press Inc., New York, 2004).

[57] A. Altland and B. D. Simons, *Condensed Matter Field Theory* (Cambridge University Press, Cambridge, England, 2010).

[58] V. Ambegaokar, U. Eckern, and G. Schön, Quantum Dynamics of Tunneling between Superconductors, Phys. Rev. Lett. **48**, 1745 (1982).

[59] Y. Makhlin, G. Schön, and A. Shnirman, Quantum-state engineering with Josephson-junction devices, Rev. Mod. Phys. **73**, 357 (2001).

[60] G. Catelani, S. E. Nigg, S. M. Girvin, R. J. Schoelkopf, and L. I. Glazman, Decoherence of superconducting qubits caused by quasiparticle tunneling, Phys. Rev. B **86**, 184514 (2012).

[61] A. O. Caldeira and A. J. Leggett, Influence of Dissipation on Quantum Tunneling in Macroscopic Systems, Phys. Rev. Lett. **46**, 211 (1981).

[62] A. Caldeira and A. Leggett, Path integral approach to quantum Brownian motion, Physica (Amsterdam) **121A**, 587 (1983).

[63] A. J. Leggett, S. Chakravarty, A. T. Dorsey, M. P. A. Fisher, A. Garg, and W. Zwerger, Dynamics of the dissipative two-state system, Rev. Mod. Phys. **59**, 1 (1987).

[64] J. Alicea, Y. Oreg, G. Refael, F. von Oppen, and M. P. A. Fisher, Non-Abelian statistics and topological quantum information processing in 1D wire networks, Nat. Phys. **7**, 412 (2011).

[65] S. N. Shevchenko, S. Ashhab, and F. Nori, Landau–Zener–Stückelberg interferometry, Phys. Rep. **492**, 1 (2010).

[66] J.-J. Feng, Z. Huang, Z. Wang, and Q. Niu, Josephson radiation from nonlinear dynamics of Majorana zero modes, Phys. Rev. B **101**, 180504(R) (2020).

[67] J. Michelsen and V. S. Shumeiko, Nonadiabatic Josephson dynamics in junctions with in-gap quasiparticles, Low Temp. Phys. **36**, 925 (2010).

[68] J. Michelsen and V. S. Shumeiko, Reentrance Effect in Macroscopic Quantum Tunneling and Nonadiabatic Josephson Dynamics in *d*-Wave Junctions, Phys. Rev. Lett. **105**, 127001 (2010).

[69] T. Gilbert, A phenomenological theory of damping in ferromagnetic materials, IEEE Trans. Magn. **40**, 3443 (2004).

[70] J. A. Sanders, F. Verhulst, and J. Murdock, *Averaging Methods in Nonlinear Dynamical Systems* (Springer, New York, 2007), Vol. 59.